

Photoacoustic wave propagating from normal into superconductive phases in Pb single crystals

Masanobu Iwanaga*

Department of Physics, Graduate School of Science, Tohoku University, Sendai 980-8578, Japan

(Received 4 April 2005; published 20 July 2005)

The photoacoustic (PA) wave has been examined in a superconductor of the first kind, a Pb single crystal. The PA wave is induced by optical excitation of an electronic state and propagates from the normal into the superconductive phase below T_c . It is clearly shown by wavelet analysis that the measured PA wave includes two different components. The high-frequency component is megahertz ultrasonic and the relatively low-frequency one is induced by a thermal wave. The latter is observed in a similar manner irrespective of T_c . On the other hand, the megahertz-frequency component is obviously enhanced below T_c . The behavior is reproduced by the change of attenuation of the longitudinal ultrasonic wave and is consistent with BCS theory.

DOI: 10.1103/PhysRevB.72.012509

PACS number(s): 74.25.Ld, 78.20.Hp, 62.80.+f

Photoacoustic (PA) spectroscopy has the special advantage of analyzing thermal and elastic signals induced by photoexcitation, and has been widely applied to gases, liquids, and solids.^{1,2} Since the PA signal detected by a piezoelectric transducer (PZT) is thermoelastic,¹ PA spectroscopy is considered effective to examine phase transitions. Indeed, PA signals around the phase-transition point were theoretically studied,^{3,4} and several observations for first- and second-order transitions have been reported so far.^{4–7} In the previous reports, the change of PA signal has not been definitely attributed to the change of a physical quantity. This is because several physical parameters can contribute to the change of PA signal. In addition, since the PA signal was usually picked up by a lock-in detector, the information is expressed by only two values, the amplitude and phase. Thus, the PA technique has advantages and disadvantages: the access to several physical quantities and the ambiguity in the interpretation. To extract more information in PA measurements, it is probably significant to examine the PA wave itself. Generally, PA waves are generated from a heat source that results from nonradiative energy relaxation of photoexcited electrons. From the generation process, PA waves are regarded as the thermal and/or elastic waves associated with energy dissipation. The PA waves are expected to include the modes peculiar to the medium. If it is true, the analysis in the time and frequency domains will be helpful to make the physical properties clear; however, this kind of study has hardly been reported.

In the PA studies to date, superconductive transitions have not been examined to our knowledge. As widely known, the transitions are second order without any crystallographic transition and are responsible for drastic change of electric conductivity. The transition has been most extensively investigated in various physical properties such as magnetic, thermal, and ultrasonic properties. Thus, a superconductor described by BCS theory⁸ seems suitable to test physical quantities detected in PA measurements. In this study, it is an aim to clarify the properties of the PA wave and signals. Moreover, it is expected to reveal how one can analyze the superconductive transition with PA spectroscopy. When photoexcitation induces an electronic interband transition, it destroys the superconductive phase because the energy is far

larger than the energy gap in the phase. The effect is also discussed.

Concretely, a Pb single crystal is explored in this study. The crystal is a superconductor of the first kind described by the strong electron-phonon-coupled BCS theory; the superconductive phase has been closely investigated with the far-infrared spectroscopy,⁹ the electron tunneling technique,¹⁰ the ultrasonic pulse-echo technique,^{11–14} and so on. The crystal has the critical temperature T_C of 7.22 K.¹⁵ Thus, various material parameters have been obtained so far.

The Pb single crystal has a purity more than 99.999% and is the size of $5 \times 5 \times 1$ mm³; the plane of 5×5 mm² is the (100) plane and the thickness is 1 mm. The PZT of the same size as the Pb single crystal was used in the PA measurement; the PZT has the resonant frequency of 4.00 MHz and the Curie point at 603 K. As drawn in Fig. 1, the (100) plane of Pb crystal was firmly attached to the 5×5 mm² plane of the PZT with conductive organic paste. Since the lead wires were also attached as shown in Fig. 1, the detected voltage is proportional to the stress along the thickness direction, and the detected PA wave is a bulk wave that propagates through the crystal. In the present configuration, the bulk wave generally includes a wave along the off-thickness direction. The specimen and PZT were set in a He-flow cryostat equipped with a temperature controller.

The incident 2.33 eV light in measuring the PA wave was the second harmonic of an yttrium aluminium garnet (YAG) laser and was injected onto a (100) plane; the pulse width was 5 ns, and the repetition was 10 Hz. The incident light is strongly absorbed by Pb single crystals because of the elec-

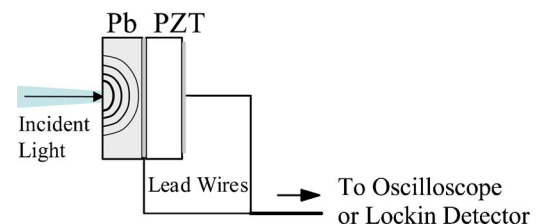


FIG. 1. (Color online) Experimental configuration. A photoacoustic (PA) wave is drawn schematically in a Pb single crystal. PZT denotes the piezoelectric transducer. Experimental parameters and conditions are described in the text.

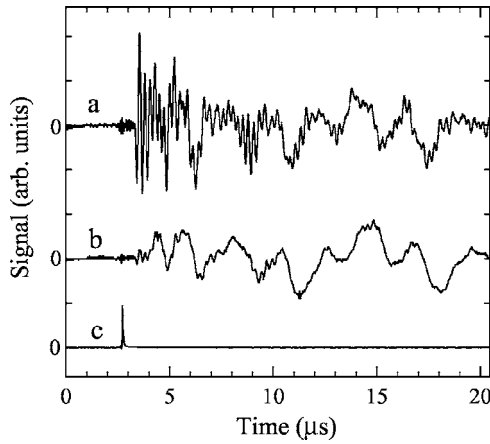


FIG. 2. Curves *a* and *b*, PA waves at 4.2 and 28.8 K, respectively. Curve *c* represents the temporal profile of an incident laser pulse detected by a photodiode; the peak indicates the time at which the laser pulse reaches the sample surface.

tronic interband transition; the absorption length is 26 nm.¹⁶ Therefore, the incident photons dissociate Cooper pairs in the thin surface layer below T_c , so that the PA wave travels from the normal into the superconductive phase. The incident light was loosely focused to a spot size of 1 mm diameter on the sample surface, and the intensity was kept at about 200 $\mu\text{J}/\text{pulse}$ in order to avoid irradiation damage on the surface.

The PA wave detected by the PZT was directly measured by an oscilloscope without any preamplifier. To examine the change of PA signal around T_c , the PA signal was stimulated with chopped continuous-wave (cw) Ar-laser light of 2.41 eV and was picked up by a two-phase lock-in detector. The incident light was loosely focused to a size of 2 mm diameter on the specimen surface, and the power was 10 mW.

Figure 2 shows the PA waves at 4.2 (curve *a*) and 28.8 K (curve *b*) in a Pb single crystal. Curve *c* in Fig. 2 displays the temporal profile of a 2.33 eV and 5 ns laser pulse, measured by a photodiode. The incident laser pulses reached the sample surface at 2.72 μs . As seen in Fig. 2, the PA wave at 4.2 K includes many sharp spikes while the wave at 28.8 K has far fewer spikes. No further fine structure of PA wave is observed by enlarging the waves at 4.2 and 28.8 K in the time domain. The difference of the two waves suggests that the PA wave at 4.2 K has a large amount of megahertz components and is indeed presented in Fig. 3 as the image plot in the time-frequency domain. Concerning the shape of PA waves, it is to be noted that the PA wave measured by PZT's, in principle, includes the multiple reflection in the crystal and the ringing in the PZT simultaneously. The effect is well discriminated below by analyzing PA wave in the time-frequency domain.

Figure 3 is the result of time-frequency-domain analysis using wavelet¹⁷ and presents the image plot of the PA wave in Fig. 2. Wavelet transformation enables us to extract the frequency component from the wave in the time domain. The method has multiresolution and is a superior extension of Fourier transformation. Figure 3(a) corresponds to the result at 4.2 K (curve *a* in Fig. 2) and Fig. 3(b) to that at 28.8 K (curve *b*). A prominent signal appears at 4 MHz only at 4.2 K

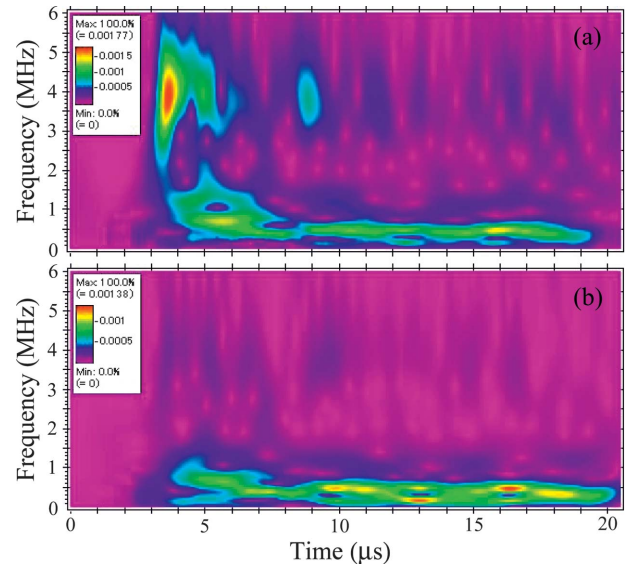


FIG. 3. (Color) Time-frequency-domain image plot of PA wave in Fig. 2: (a) 4.2 K and (b) 28.8 K. The image maps were obtained by wavelet analysis.

and the MHz component is strongly suppressed at 28.8 K. The peak position corresponds to the resonance of PZT and indicates the strong PA signal at MHz range. In this setup, a part of the strong PA signal appears prominently by the PZT resonance. On the other hand, oscillations are observed at 0.4 MHz in both image maps. The component at 0.4 MHz agrees with ringing frequency in the PZT,⁷ the ringing effect was detected in the configuration that the sample is removed in Fig. 1. Therefore, the PZT ringing is ascribed to the heat by laser irradiation. Presumably, the component at 0.4 MHz is induced by the thermal wave arrived at the interface between the crystal and PZT.

Figure 4 displays temporal profiles at 4.0 and 0.4 MHz in Fig. 3. It is apparent from Fig. 4(a) that the PA signal at 4.2 K is enhanced at 4.0 MHz while Fig. 4(b) presents that the intensity and profile of PZT ringing are similar below and above T_c . These results indicate explicitly that the two components are independent of each other; in other words, the ringing at 0.4 MHz is not induced by the MHz component. The likeness in Fig. 4(b) shows that the intensities of both waves are just proportional to the intensity of incident light and suggests that the ringing comes from a thermal wave. Furthermore, the PA signal at 4.0 MHz grows rapidly at 3.0 μs in Fig. 4(a) while the PA signal at 0.4 MHz increases gradually after 4.0 μs . The results also imply that the low-frequency component is induced by a wave different from the ultrasonic wave connected to 4.0 MHz component. Thus, taking account of the results in Figs. 3 and 4, it is probable that the PA wave includes two different physical components, ultrasonic and thermal waves.

In Fig. 5, the intensity of the PA signal (PAS) is plotted with solid circles against temperature. The PA signals were stimulated with 2.41 eV, cw laser light chopped at 104 Hz and picked up from low to high temperatures. The intensity was measured with a two-phase lock-in detector under the condition that each temperature is stable. The intensity keeps

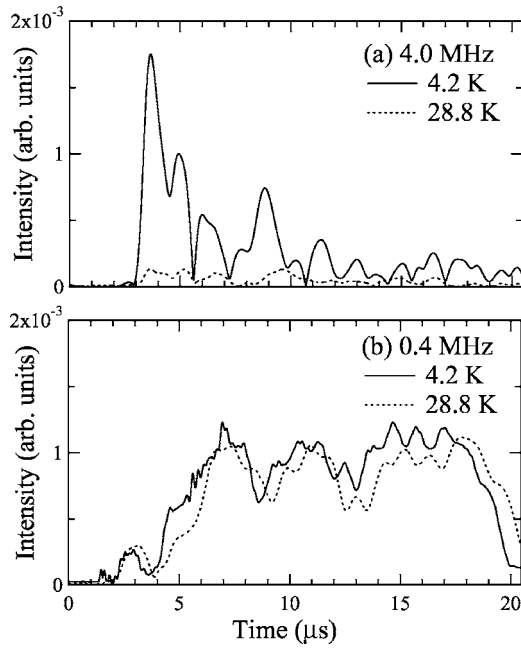


FIG. 4. Temporal profile of time-frequency plot at (a) 4.0 and (b) 0.4 MHz. The profiles are extracted from Fig. 3. Solid lines represent the profiles at 4.2 K and dotted lines at 28.8 K.

nearly constant from T_c to room temperature while it is enhanced below T_c ; the increase amount is almost in agreement with that of the 4.0 MHz component in Fig. 4(a). Thus, the PA signal picked up by the lock-in detector is ascribed to the leading component of the PA wave. The temperature profile of PAS intensity is reproduced in Fig. 5; the calculated curve (solid line) is derived as follows.

Because of the leading component of the PA wave and the present experimental configuration, it is assumed here that the PA signal in Fig. 5 comes from a longitudinal ultrasonic wave. Then, Fig. 5 can be regarded as the plot of intensity of longitudinal ultrasonic wave. In this case, the ordinate is proportional to the decayed intensity $\exp(-\alpha d)$, where α stands for the absorption coefficient of the ultrasonic wave in the crystal and d is the thickness of the crystal ($d=1.0$ mm). In the superconductive phase, the α has to be replaced with α_s ,

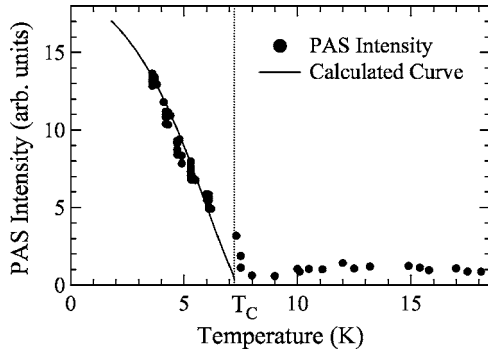


FIG. 5. The intensity of PAS (solid circles) vs temperature. T_c denotes the superconductive transition temperature of 7.22 K. Solid line is calculated combining the attenuation of longitudinal ultrasonic wave with BCS theory, and fits the measured data below T_c ; the derivation of the solid line is described in the text.

which is the absorption coefficient of the longitudinal ultrasonic wave in the superconductive phase.

To analyze the measured PAS intensity, the interface loss of signal has to be included. In fact, the PA signal decays in the crystal and moreover at the interface between the crystal and PZT. Therefore, an interface loss factor a_{int} is introduced ($a_{int} \geq 1$), and the measured PAS intensity is proportional to

$$\exp[-a_{int}\alpha_s(T)d] \quad (1)$$

for $T \leq T_c$. The a_{int} is treated as a fitting parameter below.

The values $\alpha_s(T)$ at 4.0 MHz are necessary in evaluating Eq. (1). However, the values are not available in existing literature. Therefore, another procedure is chosen. (i) First, the $\alpha_s(T)$ is evaluated by combining the absorption coefficient $\alpha_n(T)$ in the normal state with the ratio α_s/α_n derived in BCS theory.⁸ Though the absorption coefficient $\alpha_n(T)$ was reported only at 26.6 MHz (Ref. 11), the $\alpha_n(T)$ can be evaluated around T_c from the literature because the frequency dependence is known and the temperature dependence is independent of ultrasonic frequency below tens of MHz.¹⁸ Also, the ratio α_s/α_n is written such as

$$\alpha_s(T)/\alpha_n(T) = 2/\{1 + \exp[\Delta(T)/k_B T]\} \quad (2)$$

where $2\Delta(T)$ is the energy gap of the superconductive state, which is expressed as $\Delta(T)=\Delta(0)\sqrt{1-(T/T_c)^2}$,⁸ and $2\Delta(0)=4.38k_B T_c$ for Pb.¹⁵ (ii) The PAS intensity is fitted by Eq. (1) with changing a_{int} . (iii) Finally, the best fitted value is searched by varying the proportionality constant of Eq. (1).

In the fitting procedure, after a_{int} is uniquely determined, the proportionality constant multiplied by Eq. (1) is evaluated uniquely. Thus, the solid line in Fig. 5 is obtained and seems to reproduce the data below T_c fairly well.

The best fitted a_{int} is estimated to be 4.1 by using the relation $\alpha_n \propto \omega^2$. This is net interface loss and means that the PA wave is reduced at the interface. The reduction is suggestive of a nonoptimized interface coupling.

In the above analysis, the α_n is simply combined with the α_s/α_n . This assumes that the longitudinal ultrasonic wave is simply described by BCS theory and is not influenced by strong electron-phonon coupling in Pb. In fact, ultrasonic absorption coefficient at more than a few tens of megahertz deviates from the simple BCS result.¹² However, as frequency becomes lower, the coefficients get close to the values derived from BCS theory.¹² Therefore, the simple analysis using Eqs. (1) and (2) is found relevant to the PAS of 4.0 MHz. Moreover, the analysis suggests that the normal state generated by photoexcitation has little influence on the PA wave, that is, the state is induced only in a thin surface layer.

As for the strong electron-phonon coupling, it is significant to measure the transmission spectrum in the frequency domain by using calibrated PZT's. The PA wave is a kind of self-induced ultrasonic wave, and the transmission spectrum reveals the propagation mode; moreover, the mode includes the information on the electron-ultrasonic-wave interaction. The interaction has been classified with q (wave number of ultrasonic wave) and l (mean free length of electrons) phenomenologically. The transmission spectrum would enable us to analyze the ql effect quantitatively in experiment. In-

deed, the most effective ql was estimated¹² and corresponds to about 10 MHz; since the frequency is rather close to that in the present experiment, the transmission measurement seems realistic. The strong-coupling effect could be tested in detail by analyzing the transmission.

As seen in this study, the PA wave in the normal state is regarded as a thermal wave. The property of the PA wave is perhaps common in normal metals because the attenuation of the longitudinal ultrasonic wave is similar among them. In the case, the PAS detected by lock-in equipment has to be analyzed on the basis of this property.

Laser-induced acoustic waves have been reported.^{19,20} Since the comparison with the present PA study would attract interest, a few comments are made here. The laser-induced acoustic waves are induced by picosecond- or femtosecond-pulsed laser light and are extracted from the transient reflection detected with the pump-probe technique. Therefore, the acoustic signals have frequencies in the gigahertz to terahertz range and often correspond to optical phonons. The signals are induced at the laser-injected surface. The method is suitable for observing surface-layer phenomena because the attenuation of the wave is typically 1 μm and the wave cannot travel through bulk samples. On the other hand, the present PA wave has frequency of megahertz and transmits over 1 mm. The megahertz wave does not destroy Cooper pairs because the frequency is far smaller than the gap frequency determined by $2\Delta(T)$. That is, the PA wave travels in the superconductive phase. The frequency distribution of PA waves results from the ultrasonic propagation mode connected to energy dissipation. Therefore, the PA wave will

provide further insights about the propagation mode and energy transport in the superconductive phase.

In conclusion, PA waves have been explored in the time-frequency domain, so that it is clarified that the 4.0 MHz component is highly transmitted and the thermal wave is also observed as PZT ringing in the superconductive phase, while the thermal wave is dominant in the normal state. The enhancement of PAS intensity is reproduced fairly well from an analysis based on the attenuation constant of longitudinal ultrasonic waves, which satisfies the relation in BCS theory. Consequently, it is found that the PA signal below T_c is mainly composed of longitudinal ultrasonic waves in the present configuration. The enhanced frequency of the PA wave probably comes from the propagation mode of ultrasonic waves in the superconductive phase though further measurement using calibrated PZT's is necessary to determine the frequency distribution. The mode is likely associated with the effective interaction with superconductive electrons. The analysis of the temperature-dependent PA-signal intensity suggests that the normal state hardly contributes to the PA signal, that is, the breaking of the superconductive phase due to photoexcitation is restricted only to a thin surface layer in the crystal. As a result, the PA wave propagates through the superconductive phase.

I would like to express appreciation for support for the PA measurement by Professor T. Hayashi (Kyoto University). This study was supported in part by a Grant-in-Aid of the Japan Society for the Promotion of Science.

*Electronic address: iwanaga@phys.tohoku.ac.jp

¹C. K. N. Patel and A. C. Tam, Rev. Mod. Phys. **53**, 517 (1981).

²A. C. Tam, Rev. Mod. Phys. **58**, 381 (1986).

³P. Korpiun and R. Tilgner, J. Appl. Phys. **51**, 6115 (1980).

⁴J. Etxebarria, S. Uriarte, J. Fernández, M. J. Tello, and A. Gómez-Cuevas, J. Phys. C **17**, 6601 (1984).

⁵T. Somasundaram, P. Ganguly, and C. N. R. Rao, J. Phys. C **19**, 2137 (1986).

⁶S. Kojima, Jpn. J. Appl. Phys., Part 1 **27**, 226 (1988).

⁷M. Iwanaga, Phase Transitions **78**, 377 (2005).

⁸J. Bardeen, L. N. Cooper, and J. R. Schrieffer, Phys. Rev. **108**, 1175 (1957).

⁹P. L. Richards and M. Tinkham, Phys. Rev. **119**, 575 (1960).

¹⁰I. Giaever and M. Megerle, Phys. Rev. **122**, 1101 (1961).

¹¹H. E. Bömmel, Phys. Rev. **96**, 220 (1954).

¹²B. C. Deaton, Phys. Rev. Lett. **16**, 577 (1966).

¹³B. R. Tittmann and H. E. Bömmel, Phys. Rev. **151**, 178 (1966).

¹⁴W. A. Fate and R. W. Shaw, Phys. Rev. Lett. **19**, 230 (1967).

¹⁵C. Kittel, *Introduction to Solid State Physics*, 7th ed. (Wiley, New York, 1995), Chap. 12.

¹⁶H. G. Liljenvall, A. G. Mathewson, and H. P. Myers, Philos. Mag. **22**, 243 (1970).

¹⁷Wavelet transformation was carried out by using a software, AGU-Vallen wavelet produced by Vallen Systeme (Munich, Germany). The wavelet was taken to the 200th order. The software is available at URL <http://www.vallen.de>

¹⁸R. W. Morse, Phys. Rev. **97**, 1716 (1955).

¹⁹C. Thomsen, H. T. Grahn, H. J. Maris, and J. Tauc, Phys. Rev. B **34**, 4129 (1986).

²⁰T. K. Cheng, S. D. Brorson, A. S. Kazeroonian, J. S. Moodera, G. Dresselhaus, M. S. Dresselhaus, and E. P. Ippen, Appl. Phys. Lett. **57**, 1004 (1990).